Article

Pluvial Flood Risk Assessment Tool (PFRA) for Rainwater Management and Adaptation to Climate Change in Newly Urbanised Areas

Szymon Szewrański [1],* [ID], Jakub Chruściński [1], Jan Kazak [1] [ID], Małgorzata Świąder [1], Katarzyna Tokarczyk-Dorociak [2] and Romuald Żmuda [3]

[1] Department of Spatial Economy, Wrocław University of Environmental and Life Sciences, ul. Grunwaldzka 55, 50-357 Wrocław, Poland; kuba.chruscinski@gmail.com (J.C.); jan.kazak@upwr.edu.pl (J.K.); malgorzata.swiader@upwr.edu.pl (M.Ś.)

[2] Institute of Landscape Architecture, Wrocław University of Environmental and Life Sciences, ul. Grunwaldzka 55, 50-357 Wrocław, Poland; katarzyna.tokarczyk-dorociak@upwr.edu.pl

[3] Institute of Environmental Protection and Development, Wrocław University of Environmental and Life Sciences, pl. Grunwaldzki 24, 50-363 Wrocław, Poland; romuald.zmuda@upwr.edu.pl.com

* Correspondence: szymon.szewranski@upwr.edu.pl

check for updates

Abstract: The aim of this research is to develop the Pluvial Flood Risk Assessment tool (PFRA) for rainwater management and adaptation to climate change in newly urbanised areas. PFRA allows pluvial hazard assessment, as well as pluvial flood risk mapping. The original model was created using ArcGIS software with the ArcHydro extension, and the script was written using the Python programming language. The PFRA model effectively combines information about land cover, soils, microtopography (LiDAR data), and projected hydro-meteorological conditions, which enables the identification of the spatial and temporal distribution of pluvial flood risks in newly developed areas. Further improvements to the PFRA concern the quantification of pluvial flood-related damages, the application of high resolution precipitation data, and the optimisation of coding.

Keywords: pluvial flood; risk assessment; risk mapping; rainwater management; urban climate adaptation; decision support system

1. Introduction

The future of cities will be challenged by the growing number of inhabitants [1]; unsustainable suburbanisation and sprawl development [2–5]; and climate change and pluvial conditions, e.g., rainfall height and intensity, spatial and temporal distribution [6–8]. A common consequence of land development and infrastructure construction is soil sealing [9]. The more impervious the cover, the more it fosters runoff concentration and generates a higher surface water flow rate [10–12]. In conjunction with urban growth, an increase in the frequency and patterns of high intensity rainfall is expected [13]. The interplay of land cover, urban fabric density, and extreme and high-rate precipitation, which far exceed the capacity of a city's drainage systems and the urban topography, may lead to pluvial flash floods [14–16]. A pluvial flood results from intense, often convective, rainstorms, which generate a rapid overland flow and pluvial inundation. Flash flooding occurs before the rainfall runoff enters any water course or drainage system [17,18]. Urbanisation growth and observed climate trends have given rise to more frequent and severe urban pluvial flooding. As exposure and vulnerability patterns also change, the pluvial flood risk and related damages are expected to increase in the future [19,20]. A growing population density and the rising concentration of property and infrastructure increase the threat of urban flooding. In short, the more floods, the higher the

losses [21]. The overall costs related to floods are much higher when occurring in urban areas than in rural areas. In cities, relatively small floods can initiate large disruptions [13]. Additionally, Van Ootegem et al. [22] argue that pluvial floods generate fewer losses but those events are more frequent than fluvial floods. Therefore, cumulative damage cause by pluvial floods could be larger from year to year. Hammond et al. [1] distinguished between tangible and intangible flood impacts. Tangible impacts are expressed in monetary units. Data show that the level of economic losses (direct economic losses) in recent decades has increased significantly [23]. Another distinction can be made between direct and indirect impacts. Any losses caused immediately or shortly after physical contact with floodwater are recognized as direct impacts. Indirect impacts may occur beyond the location and time of a flood event, such as long-lasting trauma and stress [24]. According to Blanc et al. [14], pluvial floods bring severe damage to public and private buildings and urban infrastructure, and, in turn, affect human health and life. As 75% of future flood damages occur in urban and newly built-up areas, cities are expected to stay more resilient. Local authorities should adopt sustainable strategies for the adaptation to new climatic and socio-economic conditions [16].

The design of resilient cities and the development of the urban fabric should ideally be based on the actual data and knowledge regarding pluvial flood hazards, the potential impacts of related economic losses, and potential threats to human life and safety [1]. Therefore, pluvial flood risk assessment is necessary for rational decision making in the processes of adaptation and spatial planning [25]. A knowledge-based approach should aid the improvement of land configuration and the geometry of urban surfaces, and the architecture of buildings and streets, which play a crucial role in flow accumulation and inundation [14]. So-called best management practices (BMPs) and low impact development practices (LID) are examples of adaptation measures [9]. Such measures basically involve the on-site improvement of retention, infiltration, evaporation, and rainfall water recycling with the use of green roofs, permeable or porous pavements, rain gardening [26], urban rainwater harvesting [27], or the application of water-absorbing geocomposites [28].

Bioretention remains the most effective LID practice [7]. Some measures are referred to as Sustainable Urban Drainage Systems [29] and Water Sensitive Urban Design. The general idea behind these solutions is to disconnect the storm runoff network from the sewer network [30], mainly because the hydraulic performance of already existing urban drainage networks is insufficient for the new pluvial conditions [31]. Expanding and upgrading the conventional drainage systems are expensive procedures, and often impractical and technically impossible [10]. Thus, rainfall water should alternatively be stored on-site within a decentralized retention system rather than being discharged [12].

Urban design and decision–making in pluvial flood adaptation can be supported by risk assessment tools. Astrom et al. [32] argued that such tools have to be transparent, easy to communicate between different research fields, and be based on the best available knowledge. The system should be effective in decision-making with uncertain boundary conditions. Therefore, the analytical and decision-making process should include pluvial events modelling, hazard and risk assessment, and risk mapping, followed by strategic planning, as well as designing flood mitigation and adaptation measures [33]. All of the aforementioned steps could be complemented by simulations of changes in land use, a transition impact assessment [34], or a hydrogeological factors' evaluation [35,36].

Ahiablame and Shakya [26] developed the Personal Computer Storm Water Management Model (PCSWMM), which helps evaluate runoff and flood reduction effects of LID practices. The PCSWMM integrates the USEPA Storm Water Management Model (SWMW) engine, the Web-based Hydrograph Analysis Tool application, and the Geographic Information Systems (GIS). The SWMW model was used by Qin et al. [10] and Chen et al. [37] to evaluate the effects of LID on flood reduction. In Poland, the SWMM has been applied in the Hydrodynamic Model of Urban Drainage System [38]. Additionally, Sperotto et al. [11] designed the Regional Risk Assessment (RRA) methodology, which integrates data on future climate change scenarios. These data include the total daily precipitation provided by the RegCM4 climate model, soil humidity conditions, and information on early warnings relating to the levels of flood risk, referred to as emergency Maximum Pluvial Thresholds. The results of RRA include a set of risk and vulnerability indicators that may be used by regional decision-makers.

Apel et al. [6] proposed a combined fluvial-pluvial hazard assessment based on the probability of the occurrence of floods. The pluvial events' evaluation consists of three components: a statistical analysis of extreme rainfalls, a simulation of spatially distributed synthetic rainstorms, and the 2-D hydraulic model. The process of randomizing rainfall storm centres was completed with the use of the Monte Carlo technique for more precise simulations. The model was originally tested in the city of Can Tho in the Mekong Delta. A stochastic spatial-temporal rainfall generator was also used for pluvial flooding assessment in north-east London (UK) [19].

High-resolution and real-time pluvial modelling still remains a challenge despite advances in computing software and hardware [39]. Gregersen et al. [40] argued that predictions of short-duration extreme rainfall events should be supported by a high resolution regional climate model downscaling methodology. Schellart et al. [41] used the artificial intelligence technology of the Artificial Neural Networks (ANNs) technique as the engine for their Radar Pluvial flooding Identification for Drainage System (RAPIDS) designed for real-time forecasting. Wang et al. [42] forecast pluvial flooding over urban areas with the use of the deterministic nowcasting model provided by the UK Met Office STEPS (Short-Term Ensemble Prediction System).

The optimal use of available data sources requires a multidimensional and integrated approach, which combines pluvial hazard modelling, land vulnerably, risk assessment, and GIS mapping. The RISA project (Rain InfraStructure Adaptation) is a GIS-based methodology which offers such a comprehensive solution. It was developed for the purpose of identifying potential local flood hazards and vulnerabilities, and determining and visualising flood risk levels in a four-staged risk map [31]. Chen et al. [7] developed a planning support model named Rainwater+. Their solution combines rainwater management with computer-aided design (CAD) software, and offers a visualisation of the landscape and buildings, runoff flow paths, and directions analysis, as well as a friendly interface developed with architects and landscape designers in mind. The newly-developed City Catchment Analysis Tool (CityCAT) can be applied for designing better urban drainage and locating storm drain inlets [43].

Melo et al. [24] proposed an innovative and integrated approach for dynamic pluvial flood emergency planning. Their prototype tool supports the identification of areas that are vulnerable to floods, the identification of evacuation routes, and the calculation of the duration of the evacuation of people. Other models that are based on an integrated approach connect pluvial flood risk assessment and GIS mapping with an urban road network [44,45], optimising water management systems [12] and the economic effectiveness of flood control and adaptation measures [30,46].

There are still numerous gaps in the knowledge and research concerning pluvial flood modelling, risk assessment, and management. The assessment of pluvial flood hazards is still less frequent than fluvial flood research [6,11]. There are relatively few studies on pluvial flood damage evaluation and loss modelling [21,22]. There is no common methodology of pluvial flood hazard and risk mapping [33]. Astrom et al. [32] identified a knowledge gap in understanding future climate change scenarios and projections in decision making processes. Real-time urban flood forecasting [39] and building an early warning system [20,45] remain significant problems. Models should ideally be designed according to the spatial and temporal variability of rainfall and flood risk distribution [19]. Planners have to understand the impacts of flooding on daily life, infrastructure, transport, and property damage, and there is thus a need for new innovative measures and solutions [1]. Chen et al. [7] emphasised the lack of support tools for designers and policy-makers, which could benefit landscape management. Melo et al. [24] argued that a decision support tool should be built into the existing disaster management framework for use by civil protection authorities. Ahiablame and Shakya [26] concluded that the capabilities of the new adaption practices for flood control are not well recognised, especially for large-scale applications. In addition, Susnik et al. [30] underlined the need for quantitative assessment of the effectiveness of risk-reduction measures. Pluvial flood hazard and risk maps should be provided for large areas, even on the scale of several hundred square kilometres [47].

To sum up the review, the current gap in the knowledge and practise concerns a relatively small amount of available research on pluvial events loss quantification [21], the exclusion of climate modelling in pluvial flood risk assessment [40], and the lack of support tools for the planning of new land development [7].

2. The Aim and Scope

The aim of this study is to develop the Pluvial Flood Risk Assessment tool (PFRA) for rainwater management and adaptation to projected climate change in newly-urbanised areas. The tool is developed for spatial identification of areas vulnerable to pluvial flooding, which may overcome the limitations identified in the literature review. Pluvial flood risks are presented on risk maps. The new tools could be used to support the work of urban planners, decision makers, and landscape designers. The new model combines GIS geoprocessing, spatial analytics, terrain surface, and hydraulic analyses, as well as the results of climate change modelling. The new open source tool is to be used both in smaller and lager areas for local and regional case studies. We decided to share the code for verification in-situ to any interested parties.

3. Research and Modelling Framework

The PFRA model was created with the use of ArcGIS software with the ArcHydro extension, which serves as the basic framework for spatial analyses and modelling. The script was written in the Python programming language. The PyScripter programme was used for writing and editing the script.

3.1. PFRA Model Scheme

One of the first stages of creating the decision support model for spatial planning was to establish the conceptual principles of its architecture (Figure 1). This involved the creation of guidelines regarding the functionality of each of the system's modules, as well as a scheme showcasing their common relationships. The PFRA model makes use of spatial data to estimate the volume of surface runoff. This is followed by establishing the extent and depth values of the closed drainage areas for hydrological sinks. The model then uses the acquired information for hazard and vulnerability assessment and finally provides a risk score for local flooding.
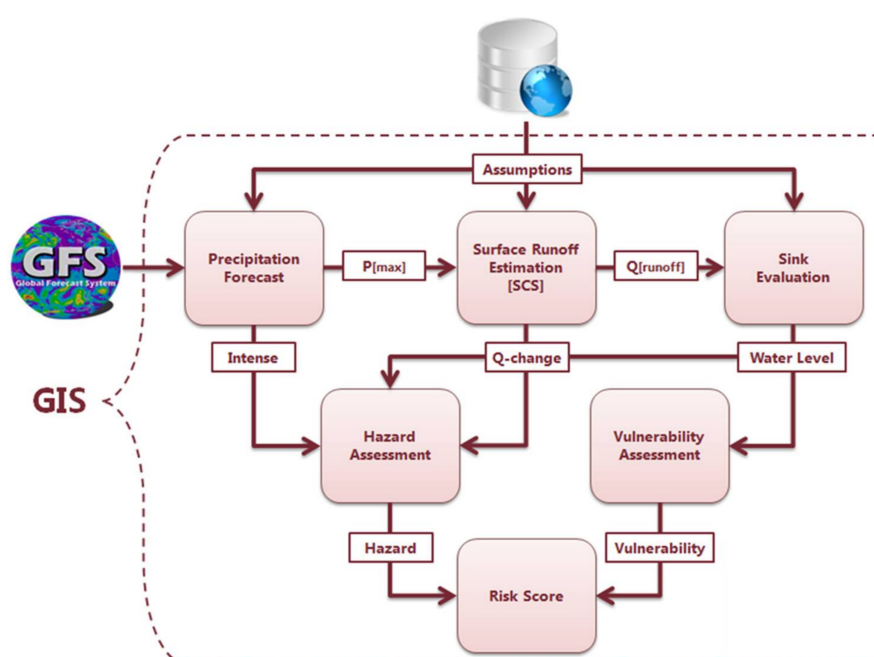

Figure 1. Research framework of Pluvial Flood Risk Assessment (PFRA).

3.2. Spatial Data Input

The input spatial data include the processing extent of the analysis; soil type and its infiltration capacity; land use and land cover; height of predicted precipitation; and topography. The principle of the model's scalability with regard to the input data was maintained in the process of its creation. Depending on the computation power of the computer, the PFRA model is capable of working on the spatial data of various resolutions and spatial scopes. This allows the model to be used both for an entire region, as well as a single record parcel. The spatial data input had to be as universal and uniform as possible for use in various European countries. It utilises land cover and land use codification from the European Urban Atlas data. The model is capable of executing computation processes using different DEM data from light detection and ranging (LiDAR) and satellite data (EU-DEM). Its only limitation in this respect is the requirement of maintaining the input file in a raster format. The final resolution of the risk assessment map depends on the quality of the input data. In the case of EU-DEM, the resolution is 25.0 m × 25.0 m, which can be used for regional studies. In the case of LiDAR, it is possible to achieve a 0.5 m × 0.5 m resolution. However, in the current model, a 1.0 m × 1.0 m grid was applied, which is more suitable for local analyses. The flood risk assessment was performed on the basis of a soil map with a reference scale of 1:25,000 (the original IUNG's soil map was updated in 2010 on a scale of 1:5000 and then generalised to 1:25,000. The soil data may be retrieved from European Environment Agency databases). The Urban Atlas land use and land cover map for 2012, which was produced using satellite images with a resolution of 2.5 m × 2.5 m, has topographic maps with a scale of 1:50,000. Spatial data were enriched by geodetic maps with a reference scale of 1:2000. In its current state, the PFRA model does not incorporate sewage systems.

3.3. Precipitation Forecast

The Precipitation Forecast model is responsible for the meteorological prognosis regarding the maximum precipitation. The programme automatically checks the maximum rainfall based on data from the Global Forecast System (GFS). The weather data are available in three-hour time steps. The script determines the time horizon of the prognosis and the maximum value of precipitation based on a shapefile generated for each time step. This value is then transferred to the Surface Runoff Estimation [SCS] module as the P[max] parameter. If the precipitation amount exceeds 25.0 mm, the Hazard Assessment module receives the Intense parameter both for the precipitation values retrieved from meteorological data or those entered manually by the user. This parameter is derived from the hazard and vulnerability assessment for residential areas [23]. Precipitation data are retrieved from the GFS model in the GRIB format, using the zyGrib software. The data then need to be converted to the shapefile format with the use of the tkdegrib programme [48]. The module is designed to operate using radar data, which allows for the full automatisation of the prognostic precipitation data retrieval process, with significantly increased data resolution and accuracy. For this purpose, the user may turn to the wradlib open source library for weather radar data processing [49].

3.4. Surface Runoff Estimation

The Surface Runoff Estimation model calculates the extent of surface runoff. The Soil Conservation Service (SCS) hydrological model is used to calculate the amount of effective precipitation. The basic intention behind this model is to use the Curve Number (CN) to determine the soil permeability for a given type of land use. This allows for the estimation of the infiltration capacity of the analysed sink at later stages. The approximate difference between the amount of precipitation and soil retention provides the size of the surface runoff defined in the model as the Q[runoff] parameter. All the design objectives of the SCS model were described in detail in Technical Release 55, "Urban Hydrology for Small Watersheds", formulated by the U.S. Department of Agriculture, Soil Conservation Service [50]. The SCS model is used in worldwide academic research, for instance, in the aforementioned Rainwater+ programme [7], the ArcCN-Runoff system [51], and in Poland [52–54]. The operations performed by

the Surface Runoff Estimation [SCS] module involve the calculation of effective rainfall. The values are then compared and properly classified (i.e., decrease, increase, or no change). The information is then passed on to the model's next module in the form of the Q-change parameter. This parameter is the result of the simple assumption that the greater the soil sealing resulting from land take, the greater the threat of pluvial flooding. The third highest value, matching the wet humidity conditions of an area with rainfall observed within the last five days, is used as the Antecendent Moisture Conditions (AMC) in the SCS model for both time horizons. The intention behind this step was to perform hydrological modelling for the worst case meteorological event scenario.

3.5. Sink Evaluation Module

The Sink Evaluation module is responsible for defining the localisation and extent of each closed drainage area. To this end, the model makes use of the Sink Evaluation tool from the ArcHydro extension. The tool determines the directions of the water runoff based on the topography raster, and designates each closed depression before translating it into parameters. The module returns a full range of information into the model, which allows for determining the area and height of the closed drainage area's bottom and crest. This is, in turn, used to calculate the volume and height of maximum filling with the input parameter of the surface runoff value. The module's output element is the Water Level parameter which contains information regarding the actual water level in each closed drainage area. The flooding area and water level in each depression change depending on the changes in the Q[runoff] parameter value. The execution of this mechanism may be represented by comparing a closed depression to an inverted cone (Figure 2).
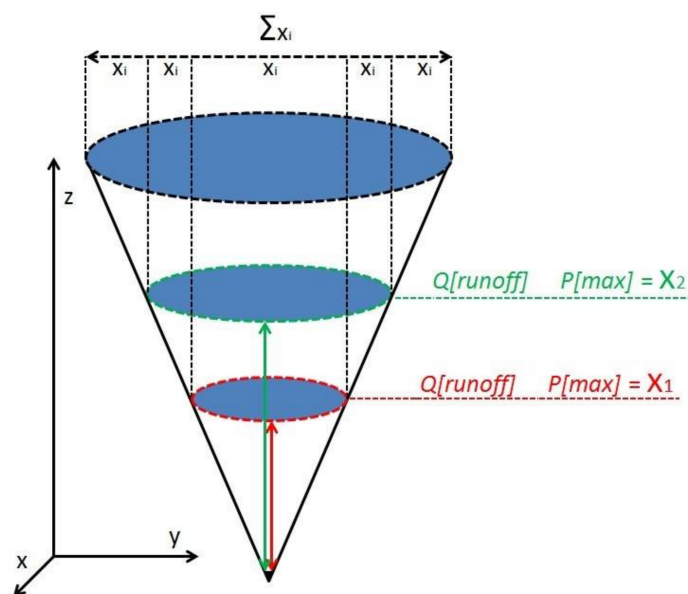

Figure 2. A representation of the relation between flooded area and amount of precipitation.

3.6. Hazard Assessment Module

The Hazard Assessment module is responsible for defining the potential threat of pluvial flooding in the studied area. Based on the literature review, we proposed a hazard formula including Intense, Q-change, and Water Level parameters. The Intense parameter has a binary value of 0 or 1. If it does not apply to the parameter's variable, 0 points are assigned. If the condition of the Intense parameter is met, i.e., when the amount of maximum precipitation exceeds 25.0 mm, the parameter variable value equals 100 points. This threshold was based on the study of Van Ootegem et al. [22]. The quantification of the Q-change parameter is done in a similar fashion. It assumes three possible values within the module. In the case of a decrease in effective precipitation, the variable assumes the

value of 0 points. If the amount of effective precipitation remains unchanged, the variable is set to 50 points. If the amount of effective precipitation increases, the variable is set to 100 points. The runoff change is calculated based on the SCS method [50]. The Water Level parameter, matching the water level expressed in centimetres, is classified in a different manner. The sum of points for the parameter increases exponentially along with the increase in the water level from 0 to 10 cm. This range had been established based on Dutch research [55]. The study analysed the average height of building entrance thresholds, and used the data to establish recommendations regarding the threat of water entering buildings. The critical value for basements was set to 0 cm, with the 10 cm stated above being the value for buildings. This parameter can vary for different constructions; however, due to good practices and standards (for instance, DIN 18065), the minimum height of an outdoor step is 12 cm. It means that the assumed 10 cm can be applied to other study regions. The module's output element is the Hazard parameter, expressing the estimated hazard value. At this stage of the research, it was decided to assume an equal influence of parameters. Therefore, the formula calculates an arithmetic mean. In future research, the possibility of using a weighted mean might be considered. The scheme of calculating the parameter may be expressed in the following Equation (1):

$$Hazard = \frac{Z_{Intense} + Z_{Q-change} + Z_{Water\ Level}}{n} \tag{1}$$

where:

$$Z_{Intense} \in \{0, 100\}$$
$$Z_{Q-change} \in \{0, 50, 100\}$$
$$Z_{Water\ Level} = \begin{cases} Water\ Level^2\ for\ 0 \leq Water\ Level \leq 10 \\ 100\ for\ Water\ Level > 10 \end{cases}$$
$$n = number\ of\ variables$$

It should be noted that the method of assessing local pluvial flood hazard used in this study is based on an original design. It is a combination of indicators used to assess flood hazard in various publications. It is impossible to directly compare and summarise those indicators, which is why prior normalisation was required. However, taking into account the open character of the PFRA model, the list itself and the way of using the indicators may be freely altered by the user in the module's source code.

3.7. Vulnerability Assessment Module

The Vulnerability Assessment model is responsible for estimating the flood vulnerability of the studied area. The module performs the estimation of the susceptibility of the studied area to flood-related damage based on the information regarding the water level from the Water Level parameter. This is achieved by using percentage rates of damage to buildings and their interiors [22], according to which each extra centimetre of water depth increases flood-related damages by 3.37% for buildings and 5.88% for furnishing. In future research, values of those coefficients might be verified for local conditions, and evaluated according to their significance to the final result of a risk assessment. The module uses these coefficients, along with the water depth retrieved from the Water Level parameter, to calculate a point product of each variable. In an analogy with the Hazard Assessment module, the arithmetic mean of two-point variables is used for the quantitative estimation of the Vulnerability output parameter. As in the hazard calculation, using a weighted mean might be considered. The manner of calculating the parameter can be expressed in the following Equation (2):

$$Vulnerability = \frac{Z_{building} + Z_{content}}{n} \tag{2}$$

where:

$$Z_{building} = \begin{cases} Water\ Level \times 3.37\ for\ 0\ \leq Water\ Level \leq 29 \\ 100\ for\ Water\ Level > 29 \end{cases}$$

$$Z_{content} = \begin{cases} Water\ Level \times 5.88\ for\ 0\ \leq Water\ Level \leq 17 \\ 100\ for\ Water\ Level > 17 \end{cases}$$

$n = number\ of\ variables$

As with the previous module, the method for assessing the vulnerability of local pluvial floods is based on an original project. Considering the open nature of this solution, the method for assessing the vulnerability or the choice of indicators may be fully modified by the user. This allows for using the model for coordinates established on the basis of local historical data.

3.8. Risk Score Module

The Risk Score module is responsible for pluvial flood risk assessment. Within this module, the programme uses the Hazard and Vulnerability input parameters to calculate the risk score for each area. For this purpose, the model uses the mathematical evaluations for controlling hazards method from the 1970s [56]. This method is still used today in many of its variations, including for the determination of the risk related to extreme weather events [11,57]. Its main principle involves the determination of a risk score based on the product of three components, namely hazard, vulnerability, and exposure. The first two parameters that are required to determine the risk score are calculated in the model's earlier modules. The exact definition of the parameter of exposition, i.e., the amount of occurrences and the exposure time of vulnerable structures to water, remains a problem. There are difficulties in properly determining the evaporation properties of water for each flooded area. The next difficulty is the so-called human factor, defined here as actions undertaken by emergency services or the inhabitants aimed at drying flooded areas. The exposition parameter, therefore, appears in the model in a simplified form. The module assigns the exposition parameter variable at 100 for each flooded area. In areas where the precipitation is fully subjected to soil retention, the module assumes the exposition parameter of 0. In order to include the risk score in a point range from 0 to 100, the module divides the product of three variables by 10000. The final method of calculating the risk score is represented in the following Equation (3).

$$Risk\ Score = \frac{Hazard\ \times\ Vulnerability \times Exposure}{10000} \tag{3}$$

where:

$Hazard = 0,\ 100$
$Vulnerability = 0,\ 100$

$$Exposure = \begin{cases} 0\ for\ Water\ Level \leq 0 \\ 100\ for\ Water\ Level > 0 \end{cases}$$

The last element of the module's operation is the execution of a reclassification based on the defined point ranges established for each risk score. Five risk scores were defined in the module with the following classification divisions:

$0 \leq$ Risk Score < 20—very low risk score
$20 \leq$ Risk Score < 40—low risk score
$40 \leq$ Risk Score < 60—medium risk score
$60 \leq$ Risk Score < 80—high risk score
$80 \leq$ Risk Score ≤ 100—very high risk score

The methodology of pluvial risk assessment varies depending on the research framework used. A superposition of the potential location-specific flood hazard level and the vulnerability level was

used to describe the potential pluvial flood risk in the city of Hamburg. The final risk levels were discretised within the risk matrix [31]. Apel et al. [6] accounted for the combined probability of fluvial and pluvial flood hazard coincidence. This combination is related to the flood risk estimation and the expected annual damages, as well as joint fluvial-pluvial hazard mapping. Astrom et al. [32] argued that the risk should be considered in the casual context in which a flood event occurs. The researchers thus proposed a five-step risk mapping process: the initiating event—trigger; control, hazard, mitigant, and consequence events. Blanc et al. [14] demonstrated how to enhance risk assessment and to improve its computation by efficient sampling and stochastic variables integration. They expressed flood consequences as economic functions relating flood depth to damages. The concept of the flood-damage function is crucial to the quantitative assessment of the flood consequences in residential areas. Residential flood damage functions (RFDF) express objects' vulnerability of structures to flooding [23]. Escuder-Bueno et al. [58] developed a comprehensive methodology of risk analysis which integrates social research survey data to hazard estimation. Economic risks are computed from the potential economic damages, land-use values, and depth-damage curves. The societal risk is related to the size of the population that is exposed to the flood event and the subsequent fatality rates. The risk analysis can be complemented by behavioural indicators [22], as well as ecological and social disruption [29].

4. Study Site

We tested the functionality of the Pluvial Flood Risk Assessment tool in the Czernica municipality (in the village of Dobrzykowice), located 12 km from the Wrocław city centre. Wrocław is the capital of the Lower Silesia region (Poland), which is regularly affected by pluvial and fluvial floods events [59]. With 636,000 inhabitants, Wrocław remains one of the largest and best developed Polish cities [60,61]. Rapid suburbanisation and sprawl processes have been recognized in Wrocław's surroundings since the political transformation of the 1990s [62–65]. In the case of the Czernica municipality, demographic changes have been observed since 1990; however, after the accession to the European Union, these changes accelerated. In 1990, the population of the municipality exceeded 6700 people and grew to almost 8600 by 2003 (an approx. increase of 27% in 13 years). And in 2016, the population reached almost 14,300 citizens (an approx. increase of 66% in 13 years). The phenomenon of urban sprawl in the Czernica municipality is still accelerating. Land transition was an effect of pursuing market economy principles in real estate trade and investment [66], and an effect of strategic decisions regarding the multifunctional development of rural areas all over the country [67]. The economic transition of rural areas was enhanced by the consecutive political and socio-cultural transformations [68,69].

The following aspects were studied with regard to Wrocław's surroundings: economic loss and real estate value fluctuation caused by suburbanisation [70,71], and the socio-cultural consequences for local communities [72]. Other aspects that were studied were the environmental aspects and impacts of urban sprawl: land take and soil sealing [73,74], water consumption increase [75], surface water pollution from new traffic infrastructure [76], low emission and air pollution [77], potential of renewable energy production [78,79], landscape diversification and conversion [80,81], and changes in ecosystem benefits and services [82,83].

From among all the identified environmental aspects, rain water management and flood risk mitigation in the city of Wrocław and its suburbia stands as one of the most important and urgent challenges for policy makers, city planners, and land developers [84,85].

The pluvial conditions in the Wrocław agglomeration were evaluated by Kotowski et al. [86]. The mean annual precipitation from the years 1881–2009 is 588.0 mm. The total annual rainfall ranged from 380.8 mm (1982) to 776.2 mm (1977). The highest daily precipitation (24h) had been recorded during extreme weather events on 17 July 1965 (115.0mm) and 10 August 1964 (110.4mm). The latest observations reported by Tokarczyk-Dorociak et al. [85] showed that on 6 June 2017, torrential rainfalls resulted in the total daily precipitation of 109.0 mm (in the Wrocław city centre). Rainfalls recorded in the city centre could have been 11% higher than in peripheral areas [85]. In this study, it is assumed

that the total amount of rainfall in the studied area should not exceed 100 mm per day, and this value was used in pluvial flood risk simulation experiments.

The simulation was conducted in a sample plot within the borders of the village of Dobrzykowice (51°05′46″ N 17°11′33″ E). The study area was 5.0 km² and this area is mainly covered by agricultural lands. Arable land with annual crops took up 46.86% of the total area, while pastures occupied 26.07%. Urban Fabric classes varied from dense development and soil sealing level (S.L), which was expressed as the percentage of the soil surface for areas covered by impervious materials (Table 1).

Table 1. Land cover pattern [%] for the study site.

Land Cover	Cover Pattern
Arable land (annual crops)	46.86%
Pastures	26.07%
Discontinuous Dense Urban Fabric (S.L.: 50–80%)	9.59%
Continuous Urban Fabric (S.L. > 80%)	4.95%
Discontinuous Very Low Density Urban Fabric (S.L. < 10%)	4.88%
Other roads and associated land	2.86%
Discontinuous Medium Density Urban Fabric (S.L.: 30–50%)	1.14%
Construction sites	1.00%
Land without current use	0.74%
Isolated Structures	0.71%
Industrial, commercial, public, military and private units	0.52%
Herbaceous vegetation associations (natural grassland. moors …)	0.35%
Green urban areas	0.20%
Discontinuous Low Density Urban Fabric (S.L.: 10–30%)	0.12%
Grand Total	100.00%

The total share of dense and medium density urban fabric is 15.68%, while low density development does not exceed 5.00%. The roads and associated lands took up 2.86% of the total area. The total open space area is approximately 75.0%, while developed land, including construction sites, is about 25%.

5. Results of the Simulation

The mean water level, as well as the risk score, depend on land cover class. The water level increases more rapidly in the first phase of a rainfall event for roads, construction sites, and industrial and commercial sites, as well as in urban areas, where the sealing level is higher than 50%. For this group, the line chart for dynamic changes in the water level in relation to the amount of precipitation can be drawn in the shape of a convex curve (blue lines). Other types of land cover are represented as more linear or concave shapes (orange lines) (Figure 3). Finally, the mean water level in green urban areas was 1.7 cm, whereas for roads and associated land it was 3.9 cm. Within the very low density urban fabric, the water level did not exceed 3.0 mm. This is quite similar to the water level recorded in pastures. A very low water level was obtained for arable land, as well as for land with no current use (Figure 4). Surprisingly, a high water level of 3.3 cm was obtained for the Discontinuous Low Density Urban Fabric (S.L.: 10–30%). In this case, the "precipitation—water level" relationship was almost linear, so that when simulated rainfall height exceeded 60 mm, the water level was still rising.

The quantification of pluvial flood risk in the studied area was the main goal of this research. Similarly, the obtained results were visualised using convex and concave curves. As observed, a risk increases rapidly in the first phase of the incidence of rainfall for roads, construction sites, commercial areas, and in densely developed urban land. The highest mean values were recorded for roads: 12.7 (Figure 5). Risk scores for construction sites and for the most sealed urban fabric ranged from 10.6 to 11.9. Very low density urban land was characterised by a risk score of 7.2; and a risk score of 7.3 was established for pastures. The risk score for arable land and land without use was lower than 6.0. The lowest values of 4.1 were observed in green urban areas. The above values represent average

levels of risk. Maximum levels were also examined (Figure 6). Overall, the highest risk of 46.3 points was recorded for the continuous 80% sealed urban fabric. Risks ranging from 30.0 to 34.0 points were observed for industrial and commercial areas, as well as for construction sites, within the dense urban fabric (S.L.: 50–80%) and for roads and associated lands. Some variability of risk scoring was observed in the case of low and medium density urban structures—the maximum risk ranged from 14.5 to 17.0 points. In areas with less than 10% soil sealing, the maximum pluvial risk did not exceed 11.0. Overall, the lowest risk was observed for arable lands.
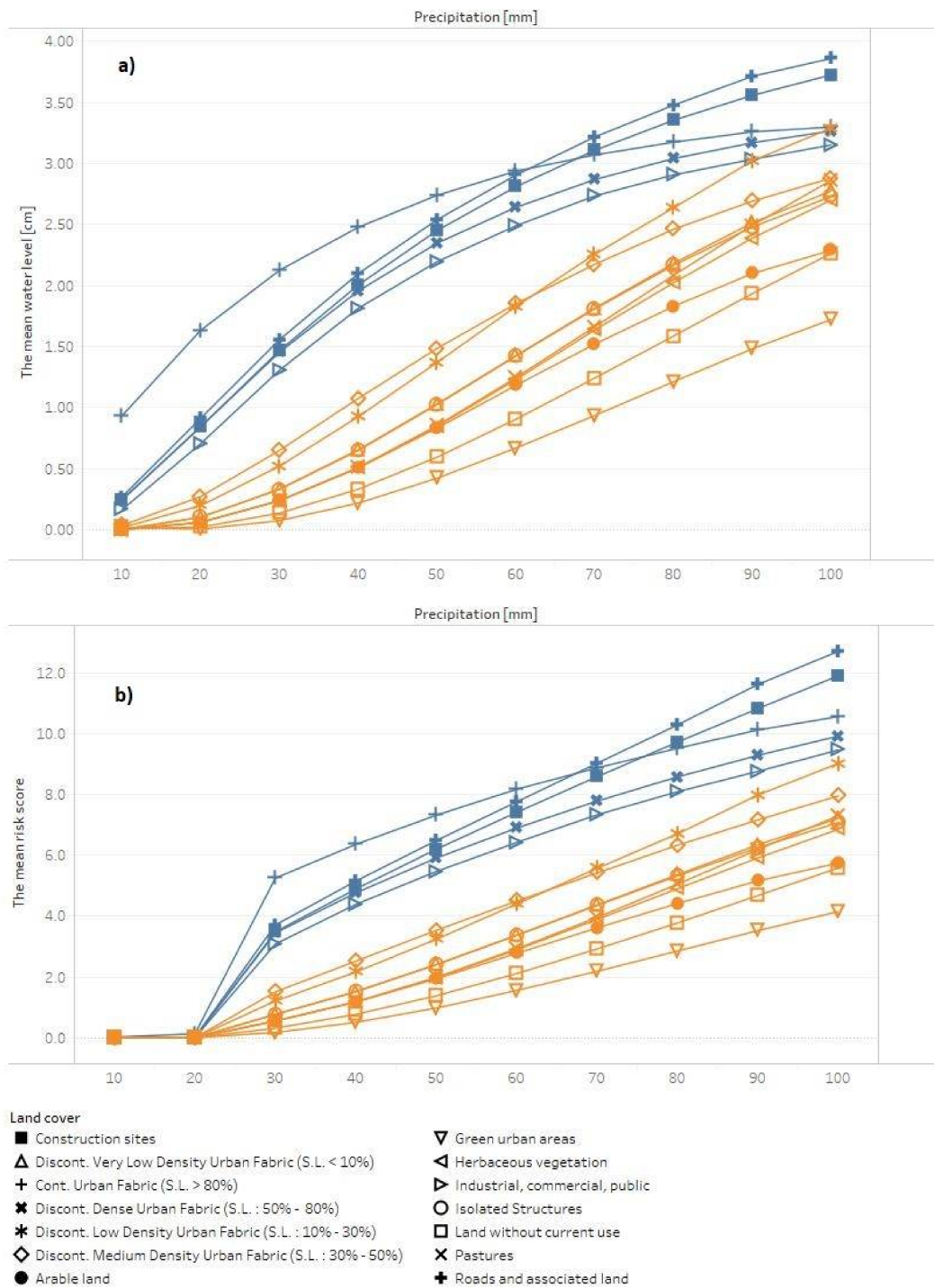

Figure 3. (**a**) The mean water level [cm] and (**b**) the mean risk score in different land cover classes according to the simulated precipitation height [mm].

Land cover	Precipitation [mm]									
	10	20	30	40	50	60	70	80	90	100
Cont. Urban Fabric (S.L. > 80%)	0.9	1.6	2.1	2.5	2.7	2.9	3.1	3.2	3.3	3.3
Roads and associated land	0.3	0.9	1.6	2.1	2.5	2.9	3.2	3.5	3.7	3.9
Discont. Dense Urban Fabric (S.L. : 50% - 80%)	0.2	0.8	1.5	2.0	2.3	2.6	2.9	3.0	3.2	3.3
Construction sites	0.2	0.8	1.5	2.0	2.5	2.8	3.1	3.4	3.6	3.7
Industrial, commercial, public	0.2	0.7	1.3	1.8	2.2	2.5	2.7	2.9	3.0	3.2
Discont. Medium Density Urban Fabric (S.L. : 30% - 50%)	0.0	0.3	0.6	1.1	1.5	1.9	2.2	2.5	2.7	2.9
Discont. Low Density Urban Fabric (S.L. : 10% - 30%)	0.0	0.2	0.5	0.9	1.4	1.8	2.3	2.6	3.0	3.3
Discont. Very Low Density Urban Fabric (S.L. < 10%)	0.0	0.1	0.3	0.7	1.0	1.4	1.8	2.2	2.5	2.8
Isolated Structures	0.0	0.1	0.3	0.6	1.0	1.4	1.8	2.2	2.5	2.7
Arable land	0.0	0.1	0.2	0.5	0.8	1.2	1.5	1.8	2.1	2.3
Pastures	0.0	0.1	0.2	0.5	0.9	1.2	1.7	2.1	2.5	2.9
Herbaceous vegetation	0.0	0.1	0.2	0.5	0.8	1.2	1.6	2.0	2.4	2.7
Land without current use	0.0	0.0	0.1	0.3	0.6	0.9	1.2	1.6	1.9	2.3
Green urban areas	0.0	0.0	0.1	0.2	0.4	0.7	0.9	1.2	1.5	1.7

Figure 4. The highlight matrix of the mean water level [cm] according to the simulated precipitation height [mm].

Land cover	Precipitation [mm]									
	10	20	30	40	50	60	70	80	90	100
Roads and associated land	0.0	0.0	3.7	5.2	6.5	7.8	9.0	10.3	11.6	12.7
Construction sites	0.0	0.0	3.5	4.9	6.2	7.4	8.6	9.7	10.8	11.9
Cont. Urban Fabric (S.L. > 80%)	0.0	0.1	5.3	6.4	7.3	8.2	8.9	9.5	10.1	10.6
Discont. Dense Urban Fabric (S.L. : 50% - 80%)	0.0	0.0	3.4	4.8	5.9	6.9	7.8	8.6	9.3	9.9
Industrial, commercial, public	0.0	0.0	3.1	4.4	5.5	6.4	7.3	8.1	8.8	9.5
Discont. Low Density Urban Fabric (S.L. : 10% - 30%)	0.0	0.0	1.2	2.2	3.2	4.4	5.6	6.7	8.0	9.0
Discont. Medium Density Urban Fabric (S.L. : 30% - 50%)	0.0	0.0	1.5	2.5	3.5	4.5	5.4	6.3	7.2	8.0
Pastures	0.0	0.0	0.6	1.2	2.0	2.9	4.0	5.1	6.2	7.3
Discont. Very Low Density Urban Fabric (S.L. < 10%)	0.0	0.0	0.8	1.5	2.4	3.4	4.4	5.4	6.3	7.2
Isolated Structures	0.0	0.0	0.8	1.5	2.4	3.4	4.4	5.3	6.3	7.1
Herbaceous vegetation	0.0	0.0	0.5	1.2	2.0	2.9	3.9	4.9	5.9	6.9
Arable land	0.0	0.0	0.6	1.2	1.9	2.8	3.6	4.4	5.2	5.7
Land without current use	0.0	0.0	0.3	0.8	1.4	2.1	2.9	3.8	4.7	5.6
Green urban areas	0.0	0.0	0.2	0.5	1.0	1.6	2.2	2.9	3.5	4.1

Figure 5. The highlight matrix of the mean pluvial flood risk scores according to simulated precipitation height [mm].
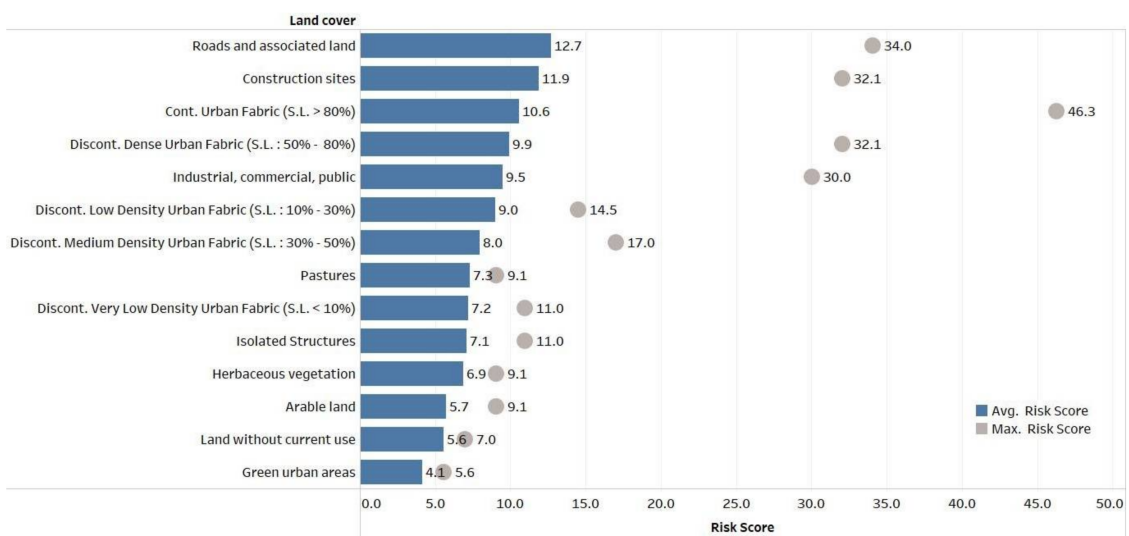

Figure 6. The mean and the maximum pluvial flood risk scores according to different land cover classes.

One of the main purposes of the Pluvial Flood Risk Assessment tool is to support spatial and flood risk management. The obtained simulation data were evaluated according to the spatial distribution of pluvial flood risk. From a practical point of view, the most important issue is to provide better extreme pluvial event control and ensure efficient warning systems in urbanised and (densely) populated areas. Thus, a clustering of all risk plots was prepared, using a k-means algorithm. The optimal number of classes was four. The cluster of the highest scores ranged from 26.0 to 46.3 (the centre point being 33.7). The next step involved the filtering of land cover data and visualising only maximum risk scores in built-up areas. The assumed thresholds can be changed optionally at any time according to specific needs.

The result is a pluvial flood risk map that can be used for location planning of new rainwater storage systems, green infrastructure facilities, or other pluvial flood control devices (Figure 7). Most areas of high risk are located in newly-developed settlements, which represent typical urban sprawl structures. High risk is noted around the main roads. One remarkable flood risk hot spot is visible in the northern part of the village, where there are numerous local roads that scored highly. Direct in situ inspections, as well as archival report studies for the spot, prove that local pluvial flooding can be accelerating as a result of unsustainable planning and land development. Verification was based on information obtained from the municipal council of Czernica. The locations of reported pluvial floods are marked by yellow dots on the flood risk map. The locations that scored in our model as high risk, but which were not identified by local authorities, are marked with red dots in Figure 7.
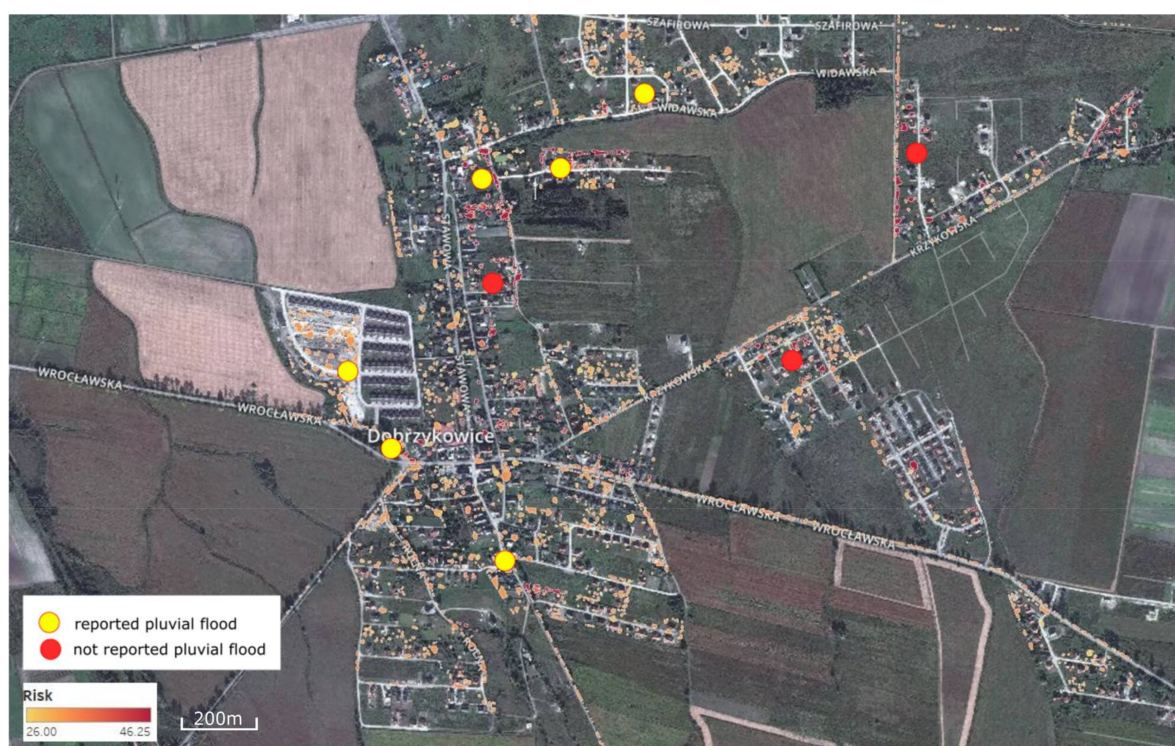

Figure 7. Spatial distribution of built-up parcels with a maximum pluvial flood risk scores of >26.0.

6. Discussion

The modelling results seem to verify the potential for using the PFRA model for a quantitative risk assessment of local pluvial floods. Using the model allows for conducting a quantified and repeatable risk assessment of pluvial floods for different time horizons. The current results correspond to the results obtained during the other studies. The results by Sperotto et al. [11] showed that the areas most vulnerable to pluvial floods are those characterised by high surface sealing and allow gradient in the

local topography. Pluvial flooding especially occurs in residential and commercial-industrial areas and infrastructures. The authors proposed a simplified approach to risk assessment, which can be applied with limited data. Thus, the model by Sperotto et al. [11] is mainly useful for indicator-based and preliminary assessments. For further research, they suggested including LiDAR data analysis and drainage system modelling, as well as the examination of water velocity, depth, and erosive capacity. The current PFRA model, as with every existing system, has certain limitations. All descriptive input file attributes and indirect calculation results from each stage are inherited in the attribute tables for output data along with the value of the risk score itself. This results in the relatively large size of the created databases, as these may contain up to a hundred columns and hundreds of thousands of records. The existing technical limitations of the geodatabases used by the ArcGIS pack applications limit the maximum number of records in the tables to over two billion. This leads to the hypothetical drawback in the model's functionality when modelling very large areas of a diverse spatial layout and input data geometry. In such cases, it is recommended to perform an initial purging of input data attribution tables, leaving only those items that are indispensable for the proper functioning of the model. Another solution used to enable large area modelling is to divide the analysis area into parts and conduct separate modelling for each of them. In the case of the PFRA model script, researchers attempted to limit the size of the input files by keeping only those attribute fields that are relevant to the modelling results. The list with the names of the retained columns is defined at the very end of the PFRA model script. Eventually, it is necessary to introduce a solution by combining all of the records with the same cell value of a given field in order to limit the probability of an error in the execution of the model. Another element affecting the proper functioning of the model is the typological accuracy of the input data. Typological errors were observed after using the soil data from national databases—loopholes and different types of soil overlapping one another. This required the use of an algorithm to remove inaccurate records and filling in the empty values based on the highest occurrence rate for each type of soil. The observed sensitivity of the modelling results to data input quality indicated the need for future implementation to have a solution which allows for the initial validation of the topology of each vector input data. This would also help avoid cases of modelling data with logical errors and would enable the automatic generation of feedback for the user. The introduction of the solutions described above may have a positive impact on the greatest limitation: the time required to execute all processes once the model is initiated. The problem of the temporal and spatial accuracy of the input data in context of model validation is widely reported.

The problem of risk mapping validation was addressed by Apel et al. [6]. They could not assess the uncertainty associated with assumptions on storm extent and spatial distribution of rainfall intensity. It was concluded that risk maps should be mainly used for the identification of the most vulnerable areas. Water depths should be taken as a rough estimation only. For future research, they suggest an evaluation of radar rainfall data. Additionally, studies on the hydraulic model and the quality of the DEM should be provided. Bhattarai et al. [21] concluded that some level of uncertainty should be accepted for the rapid and simplified calculation of the annual damage caused by pluvial floods. The precise optimisation of the damage assessment tool requires improvement of the hydrological modelling and more accurate rainfall data at a sub-daily scale. Also, Blanc et al. [14] found that the spatial characteristics of rainfall are essential in the proper flood risk estimation. They suggested the application of a non-uniform rainfall distribution to the risk computation. Grahn and Nyberg [23] argued that the availability of data on losses and risk factors is very poor. Future research should provide better pluvial flood estimation and be focused on the identification of topography, surface runoff index, drainage capacity, and sealed surfaces. Uncertainties due to the used data were underlined by Scheid et al. [31]. They proposed flood risk mapping for the city of Hamburg without the application of a detailed hydraulic simulation. The simplified solution was suitable for the initial analysis of pluvial flood risks in urban areas. It provided a solid base for the introduction of a pluvial flood risk management plan. It also was an adequate planning basis for further detailed steps in the analysis.

Currently, one of the key challenges faced by cities is their adaptation to climate change. Spatial planning, as the main form of environmental development, serves as an essential tool allowing for the implementation of the adaptation plans. It is, therefore, justified to choose target solutions enabling the assessment and comparison of the results for each adaptation mechanism, and for different time horizons. It needs to be acknowledged that the proper identification and evaluation of existing hazards always needs to come before the implementation of specific remedial action.

Ahiablame and Shakya [26] identified the effects of selected LID combinations on runoff reduction. Their simulation of the average annual runoff showed that between 2006 and 2030, the runoff will increase by 32% due to urbanisation processes. A different scenario evaluation showed that combining two or three LID practices can decrease major flood events by 36 to 55% on average. Future research on LID scenarios for flood control should be carried out within the context of policy making and economics. Thus, the selection of LID practices for a specific project will depend on site conditions, the available design area, required LID benefits, and available funds. Decision making systems should regard the effectiveness of LID practices in reducing flood risk at large scales so that systems could be based on multivariate assessments. The simulation provided by Chen et al. [7] showed that a properly designed LID is able to offset 95% of the entire rainfall. The results of their research highlighted the need for supporting tools development, especially for the early design stage.

The experiences from PFRA testing allow us to sum up the model's limitations and further research directions. First of all, there are no local coefficients quantifying pluvial flood-related damages that can be used in calculations. The model allows changing these coefficients. However, in order to do so, there is a need to conduct studies in the future to find a suitable method of calibrating those coefficients to local conditions. It should also be assessed how significantly those variables can influence the final results. Secondly, due to precipitation resolution data, the simulation was based on the assumption of uniform rainfall spatial distribution. It might be relevant to incorporate data with a higher resolution to vary those values among study area. Finally, the use of the PRFA model requires a high computing power. As the resolution of the precipitation data is being improved, this problem will increase further. Therefore, it might be necessary to check the option of optimising the code to reduce computing power needs. Due to the model being based on open source code, it may serve its users as the basis for future research and development work.

7. Conclusions

The proposed Pluvial Flood Risk Assessment is a decision support model for spatial planning at the local level. The use of the model enables local authorities to conduct a quantified and repeatable risk assessment of pluvial floods in different time horizons. This, in turn, enables the identification of the consequences and risk assessment of a specific weather event before its occurrence, which is essential for the accuracy of decisions made in a state of uncertainty. Basing the architecture of the system on the popular GIS environment allows for its easy implementation. The spectrum of uses for the model reaches beyond the example of the local flooding hazards presented in this paper.

Apart from using the model in the procedure of establishing strategic documents for urban adaptation policies, there are a number of possible applications strictly related to planning. These include localisation analyses for water retention systems and the evaluation of local spatial development project variants based on scenario methods. The information regarding the amount of water retention in each plot may be used by municipalities in fiscal calculations with regard to diversifying the amount of rainwater tax. The condition of specific real estate being exposed to the risk of local flooding may be used by insurers to estimate the amount of premiums. Last but not least, the model may be used by real estate agencies to evaluate the investment potential of each record parcel.

After feeding current precipitation data from radar prognosis into the model, it may serve as a relatively accurate tool for constant flood monitoring for disaster recovery centres. The decision

support model for spatial planning presented in this paper may provide the impetus for a discussion on risk assessment methods for local pluvial floods.

The main finding of the current study is that the PFRA model effectively combines information about land cover, soils, microtopography (LiDAR data), and projected hydro-meteorological conditions. The proposed workflow enables the identification of the spatial and temporal distribution of pluvial flood risk in newly developed areas.

Author Contributions: All authors formulated the concept. Szymon Szewrański performed the results analysis and wrote the initial version. Jakub Chruściński designed the model and developed the script. Jan Kazak and Małgorzata Świąder processed and analysed geospatial data. Katarzyna Tokarczyk-Dorociak and Romuald Żmuda contributed the suggestion of hydro-meteorological revisions.

Conflicts of Interest: The authors declare no conflict of interest.

Abbreviations

The following abbreviations are used in this manuscript:

ANNs	Artificial Neural Networks
BMPs	Best management practices
CityCAT	City Catchment Analysis Tool
DEM	Digital Elevation Model
GFS	Global Forecast System
GIS	Geographic Information Systems
GRIB	General Regularly-distributed Information in Binary form
LID	Low impact development
LiDAR	Light Detection and Ranging
PCSWMM	Personal Computer Storm Water Management Model
PFRA	Pluvial Flood Risk Assessment
RAPIDS	Radar Pluvial flooding Identification for Drainage System
RFDF	Residential Flood Damage Functions
RISA	Rain InfraStructure Adaptation
RRA	Regional Risk Assessment
SCS	Soil Conservation Service
STEPS	Short-Term Ensemble Prediction System
SWMW	Storm Water Management Model

References

1. Hammond, M.J.; Chen, A.S.; Djordjević, S.; Butler, D.; Mark, O. Urban flood impact assessment: A state-of-the-art review. *Urban Water J.* **2015**, *12*, 14–29. [CrossRef]
2. Couch, C.; Petschel-Held, G.; Leontidou, L. *Urban Sprawl in Europe: Landscape, Land-Use Change and Policy*; Wiley-Blackwell: Hoboken, NJ, USA, 2008.
3. Triantakonstantis, D.; Stathakis, D. Examining urban sprawl in Europe using spatial metrics. *Geocarto Int.* **2015**, *30*, 1092–1112. [CrossRef]
4. Altieri, L.; Cocchi, D.; Pezzi, G.; Scott, E.M.; Ventrucci, M. Urban sprawl scatterplots for urban morphological zones data. *Ecol. Indic.* **2014**, *36*, 315–323. [CrossRef]
5. Haase, D.; Kabisch, N.; Haase, A. Endless urban growth? On the mismatch of population, household and urban land area growth and its effects on the urban debate. *PLoS ONE* **2013**, *8*, e66531. [CrossRef] [PubMed]

6. Apel, H.; Trepat, O.M.; Hung, N.N.; Chinh, D.T.; Merz, B.; Dung, N.V. Combined fluvial and pluvial urban flood hazard analysis: Concept development and application to Can Tho city, Mekong delta, Vietnam. *Nat. Hazards Earth Syst. Sci.* **2016**, *16*, 941–961. [CrossRef]

7. Chen, Y.; Samuelson, H.W.; Tong, Z. Integrated design workflow and a new tool for urban rainwater management. *J. Environ. Manag.* **2016**, *180*, 45–51. [CrossRef] [PubMed]

8. Willems, P.; Arnbjerg-Nielsen, K.; Olsson, J.; Nguyen, V.T.V. Climate change impact assessment on urban rainfall extremes and urban drainage: Methods and shortcomings. *Atmos. Res.* **2012**, *103*, 106–118. [CrossRef]

9. Recanatesi, F.; Petroselli, A.; Ripa, M.N.; Leone, A. Assessment of stormwater runoff management practices and BMPs under soil sealing: A study case in a peri-urban watershed of the metropolitan area of Rome (Italy). *J. Environ. Manag.* **2017**, *201*, 6–18. [CrossRef] [PubMed]

10. Qin, H.-P.; Li, Z.-X.; Fu, G. The effects of low impact development on urban flooding under different rainfall characteristics. *J. Environ. Manag.* **2013**, *129*, 577–585. [CrossRef] [PubMed]

11. Sperotto, A.; Torresan, S.; Gallina, V.; Coppola, E.; Critto, A.; Marcomini, A. A multi-disciplinary approach to evaluate pluvial floods risk under changing climate: The case study of the municipality of Venice (Italy). *Sci. Total Environ.* **2016**, *562*, 1031–1043. [CrossRef] [PubMed]

12. Zhou, Z.N.; Qu, L.; Zou, T. Quantitative analysis of urban pluvial flood alleviation by open surface water systems in new towns: Comparing Almere and Tianjin eco-city. *Sustainability* **2015**, *7*, 13378–13398. [CrossRef]

13. Olsen, A.S.; Zhou, Q.; Linde, J.J.; Arnbjerg-Nielsen, K. Comparing methods of calculating expected annual damage in urban pluvial flood risk assessments. *Water* **2015**, *7*, 255–270. [CrossRef]

14. Blanc, J.; Hall, J.; Roche, N.; Dawson, R.; Cesses, Y.; Burton, A.; Kilsby, C. Enhanced efficiency of pluvial flood risk estimation in urban areas using spatial–temporal rainfall simulations. *J. Flood Risk Manag.* **2012**, *5*, 143–152. [CrossRef]

15. Guerreiro, S.; Glenis, V.; Dawson, R.; Kilsby, C. Pluvial flooding in European cities—A continental approach to urban flood modelling. *Water* **2017**, *9*, 296. [CrossRef]

16. Serre, D.; Barroca, B.; Diab, Y. Urban flood mitigation: Sustainable options. In *Sustainable City VI: Urban Regeneration and Sustainability*; Brebbia, C.A., Hernandez, S., Tiezzi, E., Eds.; WIT Press: Southampton, UK, 2010; Volume 129, pp. 299–309.

17. Visser, F. Rapid mapping of urban development from historic ordnance survey maps: An application for pluvial flood risk in Worcester. *J. Maps* **2014**, *10*, 276–288. [CrossRef]

18. Cobby, D.; Falconer, R.; Forbes, G.; Smyth, P.; Widgery, N.; Astle, G.; Dent, J.; Golding, B. Potential warning services for groundwater and pluvial flooding. In *Flood Risk Management: Research and Practice*; Samuels, P., Huntington, S., Allsop, W., Harrop, J., Eds.; CRC Press/Balkema: Leiden, The Netherlands, 2008; pp. 1273–1280.

19. Simões, N.E.; Ochoa-Rodríguez, S.; Wang, L.P.; Pina, R.D.; Marques, A.S.; Onof, C.; Leitão, J.P. Stochastic urban pluvial flood hazard maps based upon a spatial-temporal rainfall generator. *Water* **2015**, *7*, 3396–3406. [CrossRef]

20. Rozer, V.; Muller, M.; Bubeck, P.; Kienzler, S.; Thieken, A.; Pech, I.; Schroter, K.; Buchholz, O.; Kreibich, H. Coping with pluvial floods by private households. *Water* **2016**, *8*, 304. [CrossRef]

21. Bhattarai, R.; Yoshimura, K.; Seto, S.; Nakamura, S.; Oki, T. Statistical model for economic damage from pluvial floods in Japan using rainfall data and socioeconomic parameters. *Nat. Hazards Earth Syst. Sci.* **2016**, *16*, 1063–1077. [CrossRef]

22. Van Ootegem, L.; Verhofstadt, E.; Van Herck, K.; Creten, T. Multivariate pluvial flood damage models. *Environ. Impact Assess. Rev.* **2015**, *54*, 91–100. [CrossRef]

23. Grahn, T.; Nyberg, L. Assessment of pluvial flood exposure and vulnerability of residential areas. *Int. J. Disaster Risk Reduct.* **2017**, *21*, 367–375. [CrossRef]

24. Melo, N.; Santos, B.F.; Leandro, J. A prototype tool for dynamic pluvial-flood emergency planning. *Urban Water J.* **2015**, *12*, 79–88. [CrossRef]

25. Sun, S.A.; Djordjević, S.; Khu, S.-T. A general framework for flood risk-based storm sewer network design. *Urban Water J.* **2011**, *8*, 13–27. [CrossRef]

26. Ahiablame, L.; Shakya, R. Modeling flood reduction effects of low impact development at a watershed scale. *J. Environ. Manag.* **2016**, *171*, 81–91. [CrossRef] [PubMed]

27. Campisano, A.; Butler, D.; Ward, S.; Burns, M.J.; Friedler, E.; DeBusk, K.; Fisher-Jeffes, L.N.; Ghisi, E.; Rahman, A.; Furumai, H.; et al. Urban rainwater harvesting systems: Research, implementation and future perspectives. *Water Res.* **2017**, *115*, 195–209. [CrossRef] [PubMed]

28. Lejcus, K.; Dabrowska, J.; Garlikowski, D.; Spitalniak, M. The application of water-absorbing geocomposites to support plant growth on slopes. *Geosynth. Int.* **2015**, *22*, 452–456. [CrossRef]

29. Ellis, J.B.; Revitt, D.M.; Lundy, L. An impact assessment methodology for urban surface runoff quality following best practice treatment. *Sci. Total Environ.* **2012**, *416*, 172–179. [CrossRef] [PubMed]

30. Susnik, J.; Strehl, C.; Postmes, L.A.; Vamvakeridou-Lyroudia, L.S.; Savic, D.A.; Kapelan, Z.; Malzer, H.J. Assessment of the effectiveness of a risk-reduction measure on pluvial flooding and economic loss in Eindhoven, the Netherlands. In Proceedings of the 12th International Conference on Computing and Control for the Water Industry (CCWI2013), Perugia, Italy, 2–4 September 2013; Brunone, B., Giustolisi, O., Ferrante, M., Laucelli, D., Meniconi, S., Berardi, L., Campisano, A., Eds.; Procedia Engineering, Elsevier: Amsterdam, The Netherlands, 2014; Volume 70, pp. 1619–1628.

31. Scheid, C.; Schmitt, T.; Bischoff, G.; Hüffmeyer, N.; Krieger, K.; Waldhoff, A.; Günner, C. Gis-based methodology for pluvial flood risk analysis in Hamburg. In Proceedings of the International Conference Novatech, Lyon, France, 23–27 June 2013; pp. 23–27.

32. Astrom, H.; Hansen, P.F.; Garre, L.; Arnbjerg-Nielsen, K. An influence diagram for urban flood risk assessment through pluvial flood hazards under non-stationary conditions. *J. Water Clim. Chang.* **2014**, *5*, 276–286. [CrossRef]

33. Fritsch, K.; Assmann, A.; Tyrna, B. Long-term experiences with pluvial flood risk management. In Proceedings of the 3rd European Conference on Flood Risk Management, Lyon, France, 17–21 October 2016; Lang, M., Klijn, F., Samuels, P., Eds.; EDP Sciences—Web of Conferences: Les Ulis, France, 2016; Volume 7.

34. Wang, T.; Han, Q.; de Vries, B. A semi-automatic neighborhood rule discovery approach. *Appl. Geogr.* **2017**, *88*, 73–83. [CrossRef]

35. Hełdak, M.; Szczepański, J.; Płuciennik, M.; Stacherzak, A. Planning decisions in landslide areas. *J. Ecol. Eng.* **2016**, *17*, 218–227. [CrossRef]

36. Wan, S. A spatial decision support system for extracting the core factors and thresholds for landslide susceptibility map. *Eng. Geol.* **2009**, *108*, 237–251. [CrossRef]

37. Chen, P.-Y.; Tung, C.-P.; Li, Y.-H. Low impact development planning and adaptation decision-making under climate change for a community against pluvial flooding. *Water* **2017**, *9*, 756. [CrossRef]

38. Nowakowska, M.; Kazmierczak, B.; Kotowski, A.; Wartalska, K. Identification, calibration and validation of hydrodynamic model of urban drainage system in the example of the city of Wroclaw. *Ochr. Śr.* **2017**, *39*, 51–60.

39. Rene, J.R.; Djordjevic, S.; Butler, D.; Madsen, H.; Mark, O. Assessing the potential for real-time urban flood forecasting based on a worldwide survey on data availability. *Urban Water J.* **2014**, *11*, 573–583. [CrossRef]

40. Gregersen, I.B.; Sorup, H.J.D.; Madsen, H.; Rosbjerg, D.; Mikkelsen, P.S.; Arnbjerg-Nielsen, K. Assessing future climatic changes of rainfall extremes at small spatio-temporal scales. *Clim. Chang.* **2013**, *118*, 783–797. [CrossRef]

41. Schellart, A.; Ochoa, S.; Simões, N.; Wang, L.-P.; Rico-Ramirez, M.; Liguori, S.; Duncan, A.; Chen, A.S.; Keedwell, E.; Djordjevic, S. Urban Pluvial Flood Modelling with Real Time Rainfall Information–UK Case Studies. In Proceedings of the 12nd International Conference on Urban Drainage, Porto Alegre, Brazil, 10–15 September 2011.

42. Wang, L.P.; Simoes, N.; Rico-Ramirez, M.; Ochoa, S.; Leitao, J.; Maksimovic, C. Radar-based pluvial flood forecasting over urban areas: Redbridge case study. In *Weather Radar and Hydrology*; Moore, R.J., Cole, S.J., Illingworth, A.J., Eds.; IAHS Press: Wallingford, UK, 2012; Volume 351, pp. 632–637.

43. Bertsch, R.; Glenis, V.; Kilsby, C. Urban flood simulation using synthetic storm drain networks. *Water* **2017**, *9*, 925. [CrossRef]

44. Yin, J.; Yu, D.; Wilby, R. Modelling the impact of land subsidence on urban pluvial flooding: A case study of downtown Shanghai, China. *Sci. Total Environ.* **2016**, *544*, 744–753. [CrossRef] [PubMed]

45. Yin, J.; Yu, D.; Yin, Z.; Liu, M.; He, Q. Evaluating the impact and risk of pluvial flash flood on intra-urban road network: A case study in the city center of Shanghai, China. *J. Hydrol.* **2016**, *537*, 138–145. [CrossRef]

46. Susnik, J.; Strehl, C.; Postmes, L.A.; Vamvakeridou-Lyroudia, L.S.; Malzer, H.J.; Savic, D.A.; Kapelan, Z. Assessing financial loss due to pluvial flooding and the efficacy of risk-reduction measures in the residential property sector. *Water Resour. Manag.* **2015**, *29*, 161–179. [CrossRef]

47. Tyrna, B.; Assmann, A.; Fritsch, K.; Johann, G. Large-scale high-resolution pluvial flood hazard mapping using the raster-based hydrodynamic two-dimensional model floodareahpc. *J. Flood Risk Manag.* **2017**. [CrossRef]

48. Krasowski, W. *The Possibilities of Using Quantum GIS in Visualization, Geoprocessing and Analyzing Prognostic Meteorological Data*; Wrocław University of Science and Technology: Wrocław, Poland, 2011; p. 70.

49. Heistermann, M.; Jacobi, S.; Pfaff, T. Technical note: An open source library for processing weather radar data wradlib. *Hydrol. Earth Syst. Sci.* **2013**, *17*, 863–871. [CrossRef]

50. Cronshey, R. *Urban Hydrology for Small Watersheds*; U.S. Department of Agriculture, Soil Conservation Service, Engineering Division: Washington, DC, USA, 1986.

51. Zhan, X.; Huang, M.-L. ArcCN-runoff: An ArcGIS tool for generating curve number and runoff maps. *Environ. Model. Softw.* **2004**, *19*, 875–879. [CrossRef]

52. Banach, W. Influence of raster Corine Land Cover map use on average CN value in SCS model. *Czasopismo Techniczne Środowisko* **2012**, *R.109, z.1-Ś*, 3–11.

53. Miler, A. Ocena wpływu zmian użytkowania terenu na odpływy wezbraniowe przy użyciu metody scs-cn. *Rocznik Ochrona Środowiska* **2012**, *14*, 512–524.

54. Banasik, K. *Computation of Flood Hydrographs for Small Urban Catchments*; Wydawnictwo SGGW: Warszawa, Poland, 2009; p. 27.

55. Stone, K.; Daanen, H.; Jonkhoff, W.; Bosch, P. *Quantifying the Sensitivity of our Urban Systems: Impact Functions for Urban Systems*; Knowledge for Climate Programme Office: Utrecht, The Netherlands, 2013.

56. Fine, W.T. *Mathematical Evaluations for Controlling Hazards*; Naval Ordnance Laboratory: White Oak, MD, USA; National Technical Information Service [Distributor]: Silver Spring, MD, USA; Springfield, VA, USA, 1971.

57. Cardona, O.D.; Van Aalst, M.K.; Birkmann, J.; Fordham, M.; Mc Gregor, G.; Rosa, P.; Pulwarty, R.S.; Schipper, E.L.F.; Sinh, B.T.; Décamps, H.; et al. Determinants of risk: Exposure and vulnerability. In *Managing the Risks of Extreme Events and Disasters to Advance Climate Change Adaptation: Special Report of the Intergovernmental Panel on Climate Change*; Cambridge University Press: Cambridge, UK, 2012; pp. 65–108.

58. Escuder-Bueno, I.; Castillo-Rodríguez, J.T.; Zechner, S.; Jöbstl, C.; Perales-Momparler, S.; Petaccia, G. A quantitative flood risk analysis methodology for urban areas with integration of social research data. *Nat. Hazards Earth Syst. Sci.* **2012**, *12*, 2843–2863. [CrossRef]

59. Piepiora, Z.; Kachniarz, M.; Babczuk, A. Financing the counteraction of natural disasters' effects in Lower Silesian voivodeship. In Proceedings of the 2015 International conference on Management Engineering and Management Innovation, Changsha, China, 10–11 January 2015; Wang, M., Ed.; Atlantis Press: Paris, France, 2015; Volume 3, pp. 215–220.

60. Ksiazek, S.; Suszczewicz, M. City profile: Wroclaw. *Cities* **2017**, *65*, 51–65. [CrossRef]

61. Przybyła, K.; Kulczyk-Dynowska, A.; Kachniarz, M. Quality of life in the regional capitals of Poland. *J. Econ. Issues* **2014**, *48*, 181–196. [CrossRef]

62. Warczewska, B. Przemiany przestrzenne wybranych wsi leżących w strefie podmiejskiej Wrocławia. In *Gospodarka Przestrzenna XI*; Korenik, S., Przybyła, Z., Eds.; Wydawnictwo Katedra Gospodarki Przestrzennej i Administracji Samorządowej Wydział Nauk Ekonomicznych Uniwersytet Ekonomiczny we Wrocławiu: Wrocław, Poland, 2008; pp. 327–339.

63. Gonda-Soroczynska, E. Suburbia Wrocławia a urbanizacja. In *Gospodarka Przestrzenna XI*; Korenik, S., Przybyła, Z., Eds.; Wydawnictwo Katedra Gospodarki Przestrzennej i Administracji Samorządowej Wydział Nauk Ekonomicznych Uniwersytet Ekonomiczny we Wrocławiu: Wrocław, Poland, 2008; pp. 99–109.

64. Zathey, M. *Wrocławska Strefa Suburbialna. Zmiany Morfologiczne, Funkcjonalne i Społeczne.* Ph.D. Thesis, Uniwersytet Wrocławski, Wrocław, Poland, 2005.

65. Masztalski, R. The phenomenon of the suburbanization of Wroclaw. *Int. J. Hous. Sci. Appl.* **2002**, *26*, 133–140.

66. Forys, I.; Putek-Szelag, E. Methods of linear ordering in estimation of potential of polish market of agricultural property. *Actual Probl. Econ.* **2014**, *151*, 542–550.

67. Woch, F.; Hernik, J.; Linke, H.; Sankowski, E.; Bęczkowska, M.; Noszczyk, T. Renewable energy and rural autonomy: A case study with generalizations. *Pol. J. Environ. Stud.* **2017**, *26*, 2823–2832. [CrossRef]

68. Furmankiewicz, M.; Macken-Walsh, Á. Government within governance? Polish rural development partnerships through the lens of functional representation. *J. Rural Stud.* **2016**, *46*, 12–22. [CrossRef]

69. Furmankiewicz, M.; Thompson, N.; Zielińska, M. Area-based partnerships in rural Poland: The post-accession experience. *J. Rural Stud.* **2010**, *26*, 52–62. [CrossRef]

70. Hełdak, M.; Płuciennik, M. Costs of urbanisation in Poland, based on the example of Wroclaw. In *IOP Conference Series: Materials Science and Engineering*; WMCAUS: Prague, Czech Republic, 2017; Volume 245, p. 072003.

71. Litynski, P.; Holuj, A. Urban sprawl costs: The valuation of households' losses in Poland. *J. Settl. Spat. Plan.* **2017**, *8*, 11–35. [CrossRef]

72. Kajdanek, K. Newcomers vs. Old-timers? Community, cooperation and conflict in the post-socialist suburbs of Wroclaw, Poland. In *Mobilities and Neighbourhood Belonging in Cities and Suburbs*; Watt, P., Smets, P., Eds.; Palgrave Macmillan: London, UK, 2014; pp. 182–199.

73. Szewrański, S.; Kazak, J.; Żmuda, R.; Wawer, R. Indicator-based assessment for soil resource management in the Wroclaw larger urban zone of Poland. *Pol. J. Environ. Stud.* **2017**, *26*, 2239–2248. [CrossRef]

74. Hełdak, M.; Raszka, B.; Szczepanski, J. Design of ground surface sealing in the spatial policy of communes. In Proceedings of the World Multidisciplinary Civil Engineering-Architecture-Urban Planning Symposium 2016 (WMCAUS 2016), Prague, Czech Republic, 13–17 June 2016; Drusa, M., Yilmaz, I., Marschalko, M., Coisson, E., Segalini, A., Eds.; Elsevier Science BV: Amsterdam, The Netherlands, 2016; Volume 161, pp. 1367–1372.

75. Kazak, J.; Szewrański, S. *Indicator-Based Environmental Assessment of Spatial Planning with the Use of Community Viz*; Vsb-Technical University of Ostrava: Ostrava, Czech Republic, 2013; pp. 163–173.

76. Paweska, K.; Bawiec, A.; Pulikowski, K. Wastewater treatment in submerged aerated biofilter under condition of high ammonium concentration. *Ecol. Chem. Eng. S* **2017**, *24*, 431–442. [CrossRef]

77. Żyromski, A.; Biniak-Pieróg, M.; Burszta-Adamiak, E.; Zamiar, Z. Evaluation of relationship between air pollutant concentration and meteorological elements in winter months. *J. Water Land Dev.* **2014**, *22*, 25–32. [CrossRef]

78. Kazak, J.; van Hoof, J.; Szewranski, S. Challenges in the wind turbines location process in Central Europe—the use of spatial decision support systems. *Renew. Sustain. Energy Rev.* **2017**, *76*, 425–433. [CrossRef]

79. Świąder, M.; Tokarczyk-Dorociak, K.; Szewrański, S.; Kazak, J. Analiza zapisów regionalnych programów operacyjnych w latach 2014–2020 w kontekście finansowania inwestycji z zakresu OZE. *Rynek Energii* **2016**, *Nr 3*, 72–80.

80. Tokarczyk-Dorociak, K.; Kazak, J.; Szewrański, S. Delimitacja jednostek krajobrazowych w celu wstępnej identyfikacji krajobrazów strefy podmiejskiej Wrocławia. *Infrastruktura i Ekologia Terenów Wiejskich* **2017**, *Nr I/2*, 371–384.

81. Solecka, I.; Sylla, M.; Świąder, M. Urban sprawl impact on farmland conversion in suburban area of Wrocław, Poland. In *IOP Conference Series: Materials Science and Engineering*; WMCAUS: Prague, Czech Republic, 2017; Volume 245, p. 072002.

82. Raszka, B.; Kalbarczyk, E. Methodological assumptions made in research into the benefits of ecosystem services in protected areas in the suburbs of Wroclaw, Poland. In Proceedings of the 2013 International Conference on Advances in Social Science, Humanities, and Management, Guangzhou, China, 14–15 December 2013; Kim, Y., Ed.; Atlantis Press: Paris, France, 2013; Volume 43, pp. 1–6.

83. Sylla, M. Mapping and assessment of the potential to supply selected ecosystem services at a sub-regional scale. The example of Wroclaw and its surrounding municipalities. *Ekonomia i Środowisko* **2016**, *4*, 87–98.

84. Szewrański, S.; Kazak, J.; Szkaradkiewicz, M.; Sasik, J. Flood risk factors in suburban area in the context of climate change adaptation policies—Case study of Wroclaw, Poland. *J. Ecol. Eng.* **2015**, *16*, 13–18. [CrossRef]

85. Tokarczyk-Dorociak, K.; Walter, E.; Kobierska, K.; Kołodyński, R. Rainwater management in the urban landscape of Wroclaw in terms of adaptation to climate changes. *J. Ecol. Eng.* **2017**, *18*, 171–184. [CrossRef]

86. Kotowski, A.; Dancewicz, A.; Kazmierczak, B. Distribution of precipitation in the city of Wroclaw. *Ochr. Sr.* **2010**, *32*, 37–46.